Antiviral Research 164 (2019) 147–153

Contents lists available at ScienceDirect

Antiviral Research

journal homepage: www.elsevier.com/locate/antiviral

Identification of small molecule inhibitors targeting the Zika virus envelope protein

Jared Pitts[a], Chih-Yun Hsia[a], Wenlong Lian[a], Jinhua Wang[b,c], Marc-Philipp Pfeil[a], Nicholas Kwiatkowski[b,c], Zhengnian Li[b,c], Jaebong Jang[b,c], Nathanael S. Gray[b,c], Priscilla L. Yang[a,*]

[a] Department of Microbiology and Blavatnik Institute, Harvard Medical School, 77 Avenue Louis Pasteur, Boston, MA 02115, USA
[b] Department of Cancer Biology, Dana-Farber Cancer Institute, 360 Longwood Ave, Boston, MA 02215, USA
[c] Department of Biological Chemistry and Molecular Pharmacology, Harvard Medical School, 360 Longwood Ave, Boston, MA 02215, USA

ABSTRACT

The recent emergence of Zika virus, a mosquito-borne flavivirus, in the Americas has shed light on the severe neurological diseases associated with infection, notably congenital microcephaly in newborns and Guillain-Barré syndrome in adults. Despite the recent focus on Zika virus, there are currently no approved vaccines or antiviral therapies available to treat or prevent infection. In this study we established a competitive amplified luminescent proximity homogeneous assay (ALPHAscreen) to identify small molecule inhibitors targeting the envelope protein of Zika virus (Zika E). We utilized this assay to screen two libraries of nearly 27,000 compounds and identified seven novel inhibitors of Zika E. Characterization of these primary screening leads demonstrated that inhibition of Zika virus occurs at non-cytotoxic concentrations for all seven lead compounds. In addition, we found that all seven lead compounds have potent activity against the closely related dengue virus 2 but not vesicular stomatitis virus, an unrelated enveloped virus. Biochemical experiments indicate that these compounds act by preventing E-mediated membrane fusion. This work highlights a new method for the discovery and optimization of direct-acting antivirals targeting the E protein of Zika and other flaviviruses.

Zika virus (ZIKV) is a mosquito-borne virus belonging to the Flavivirus genus, which includes the closely related dengue, Japanese encephalitis, and yellow fever viruses (DENV, JEV, and YFV, respectively). The outbreak of ZIKV in 2015–2016 is estimated to have caused over 500,000 cases throughout Central and South America (Pan-American Health Organization/World Health Organization Zika report). Symptomatic ZIKV infections commonly result in fever with associated rash, conjunctivitis, and joint pain but have also been associated with severe neuropathies including Guillain-Barre syndrome in adults and microcephaly in children born to infected mothers. ZIKV has been observed to establish long-term infections in the testis (Govero et al., 2016; Ma et al., 2016), and continued detection of ZIKV in body fluids (*e.g.*, semen, saliva, breast milk) for weeks to months after the onset of symptoms (Calvet et al., 2018; Paz-Bailey et al., 2017) indicates a need for interventions to reduce viral burden due to replication in these sites and to thereby reduce transmission via alternative mechanisms (*e.g.*, breastfeeding or sexual).

There are effective flaviviral vaccines against YFV, JEV, and tick-borne encephalitis virus (TEV), however Dengvaxia, currently the only marketed DENV vaccine, not only fails to elicit protective immunity in those lacking prior DENV exposure but also increases the risk of severe disease in these individuals, likely due to antibody-dependent enhancement of infection (Capeding et al., 2014; Hadinegoro et al., 2015; Sabchareon et al., 2012; Halstead and Russell, 2016; Halstead, 2016; Villar et al., 2015). Although early results towards a ZIKV vaccine are promising (Gaudinski et al., 2018; Modjarrad et al., 2018), the cross-reactivity of ZIKV and DENV antibodies has been shown to enhance infection and disease in cell culture and murine models (Fowler et al., 2018; Sapparapu et al., 2016; Stettler et al., 2016; Zimmerman et al., 2018). Due to the potential challenges this phenomenon may present to vaccine safety and efficacy, antivirals may provide a complementary strategy to limit ZIKV viral burden, viral persistence, and disease severity without the risk of cross-reactive antibodies. The direct-acting antivirals that now cure chronic hepatitis C virus (HCV, Family: Flaviviridae; genus: Hepacivirus) provide precedent for the use of direct-acting antivirals against members of this viral family. Despite this, multiple efforts to develop antivirals against the polymerase and protease proteins of dengue and other flaviviruses have been unsuccessful in advancing candidates to the clinic (Boldescu et al., 2017; Lim, 2019). Consequently, complementary efforts against alternative antiviral targets remain of high interest and value.

The flavivirus envelope protein, E, mediates the initial attachment

* Corresponding author.
E-mail address: priscilla_yang@hms.harvard.edu (P.L. Yang).

https://doi.org/10.1016/j.antiviral.2019.02.008
Received 21 December 2018; Received in revised form 10 February 2019; Accepted 12 February 2019
Available online 13 February 2019
0166-3542/

of the virion to the host cell membrane through interaction with cell surface attachment factors (*e.g.*, DC-SIGN, Tim/Tam family phosphatidylserine receptors) (Hamel et al., 2015; Tassaneetrithep et al., 2003). Following internalization of the virion via a clathrin-dependent process, endosomal acidification triggers significant structural changes in E that drive fusion of the viral and endosomal membranes. This creates a fusion pore that releases the viral RNA genome into the cytoplasm where viral gene expression and replication ensue. We previously identified several classes of small molecule antivirals that bind a pocket between domains I and II of the prefusion, dimeric form of DENV E present on virions and inhibit E-mediated membrane fusion (Clark et al., 2016; Schmidt et al., 2012; de Wispelaere et al., 2018). Due to partial conservation of this site, a subset of DENV E inhibitors also inhibit other flaviviruses including ZIKV, while others appear to be selective for DENV (Lian et al., 2018; de Wispelaere et al., 2018). We recently established a competitive amplified luminescent proximity homogeneous assay (ALPHAscreen) to enable target-based discovery and optimization of inhibitors of DENV2 E and showed this to be a reliable tool for identifying new scaffolds that inhibit DENV infectivity through the same biochemical mechanism of action (*i.e.*, inhibition of E-mediated fusion) (Lian et al., 2018). Here, we report the development of an analogous competitive ALPHAscreen for Zika E and a pilot high-throughput screening effort leading to discovery and characterization of seven new chemical series that inhibit ZIKV by directly targeting Zika E.

To establish a target-based assay using recombinant, soluble Zika E (ZIKV sE), we first screened biotinylated derivatives of our previously identified pyrimidine (Clark et al., 2016; de Wispelaere et al., 2018) inhibitors of DENV E (Supporting Fig. 1) to identify an appropriate ALPHAscreen probe for Zika E. Biotinylated inhibitors were immobilized on streptavidin-coated donor beads and incubated with Ni-NTA acceptor beads to which soluble, recombinant Zika E had been bound (Fig. 1A). We found that the probe based on 4,6-disubstituted pyrimidine GNF-2 ("GNF-2-biotin") consistently produced the highest signal-to-background ratio (Fig. 1B and Supporting Fig. 1). Cross-titration of protein and probe concentrations to maximize signal-to-background and competition in the presence of validated Zika E inhibitor 3-110-22 (de Wispelaere et al., 2018) established optimized conditions of 50 nM ZIKV sE and 100 nM GNF-2-biotin (Fig. 1C), yielding Z′ value of 0.63 with coefficient of variation of 4% for DMSO and 7.5% for 3-110-22, which consistently reduced ALPHAscreen signal by ~75%.

With these optimized ALPHAscreen conditions, we conducted a high-throughput screen against the commercially available Asinex 2 (macrocycles) and Asinex 3 (nucleoside analogues) libraries (https://iccb.med.harvard.edu/commercial-libraries), totaling 26,954 compounds screened at a final concentration of 30 μM (compound:-target ~ 600:1). Plate statistics for the Zika E screen had coefficients of variation ranging from 1.341 to 11.257, with 90% of the plates between 2.0 and 4.5. Z′ values ranged from 0.51 to 0.90, with most plates exhibiting a Z′ > 0.7 and signal-to-background values of ~4.

We used normalized percent inhibition (NPI) compared to the 3-110-22 positive control to identify 263 active compounds (0.97% of the total library) (Fig. 2). For the nucleoside analogue library, active compounds had an NPI > 60% ("hit" rate of 0.25%) while the macrocycle library cut-off was set at NPI > 80% ("hit" rate of 1.3%). Of these compounds, several had similar chemical structures. This suggested specific activity attributed to shared chemical structure and enabled us to focus our follow-up efforts on 106 compounds by choosing only a subset of compounds from each chemical series.

We first sought to validate that the compounds had concentration-dependent activity against recombinant ZIKV sE. IC_{50} values, defined as the compound concentration at which the ALPHAscreen signal was reduced by 50%, were determined by non-linear regression analysis of dose-response experiments. 102 of the 106 initial hit compounds exhibit IC_{50} < 30 μM, for a validation percentage of 96% (Supporting Table 1). We next performed plaque reduction neutralization tests ($PRNT_{50}$) to determine whether activity in the biochemical assay is associated with antiviral activity. To ensure that we identified compounds that inhibit ZIKV by blocking E's function in viral entry versus compounds that inhibit ZIKV via other mechanisms or targets, the compound was pre-incubated with the viral inoculum (~200 PFU, MOI of 0.005) and was present during an initial one hour infection but was otherwise absent during the assay (Supporting Fig. 2). Notably, 96 of the 106 compounds exhibit significant antiviral activity with $PRNT_{50}$ values less than 30 μM (compound:target ~ 10^8:1) (Supporting Table 1), confirming that the target-based assay identifies compounds

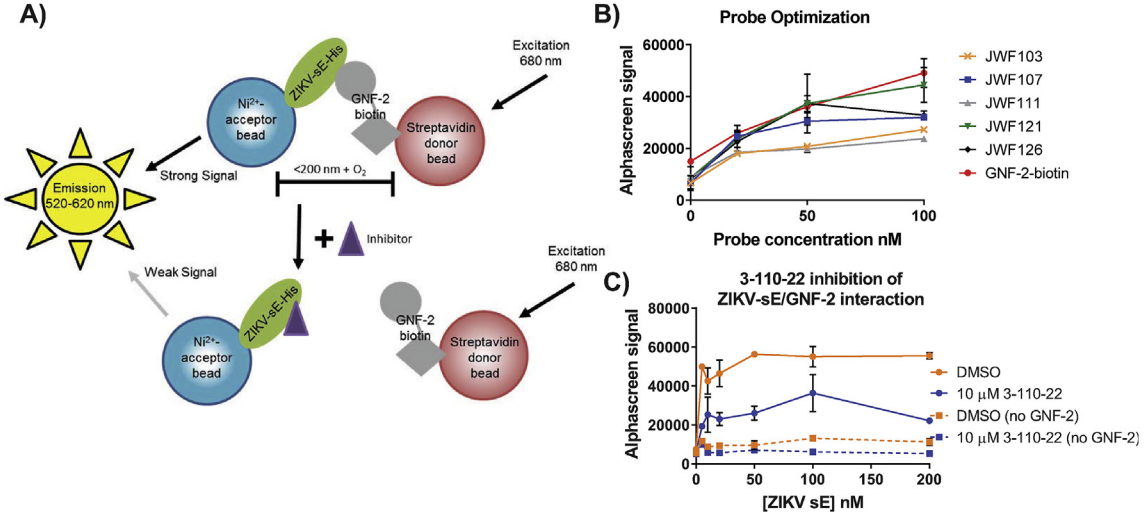

Fig. 1. Optimization of Competitive ALPHAscreen for Zika virus sE. (A) Schematic of the competitive ALPHAscreen utilized in the high-throughput screening. Compounds that interfere with the GNF-2-biotin/ZIKV sE interaction cause reduced signal and are identified as "hits." **(B)** Candidate biotinylated probes were titrated from 0 to 100 nM in the presence of 50 nM ZIKV-sE. ALPHAscreen signal is plotted as a function of probe concentration with representative data for $n \geq 2$ independent experiments shown. Error bars represent standard deviation of 3 technical replicates within the representative experiment. GNF-2-biotin provided the highest signal-to-noise across the titration. **(C)** Known DENV and ZIKV E inhibitor 3-110-22 served as a positive control and successfully reduces the ALPHAscreen signal across the ZIKV-sE titration (from 0 to 200 nM) in the presence of 100 nM GNF-2-biotin. The optimal signal reduction is observed at 50 nM ZIKV-sE and 100 nM GNF-2-biotin, and these conditions were utilized for high-throughput screening. Representative data for $n \geq 2$ independent experiments shown; error bars represent the standard deviation of 3 technical replicates within the experiment shown.

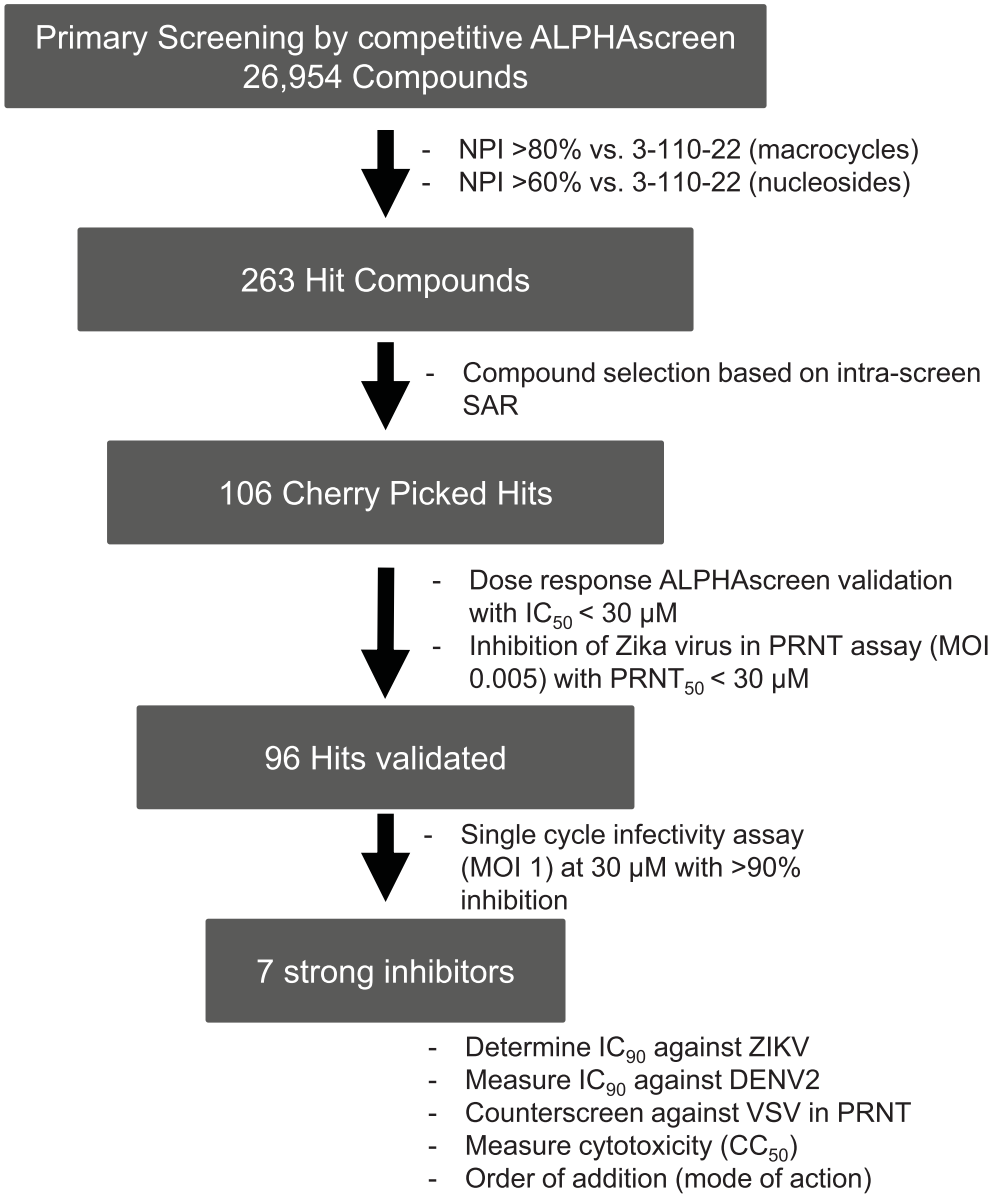

Fig. 2. Screening progression and validation. High-throughput screening and validation of screening "hits" followed the progression outlined in the flow chart. From the nearly 27,000 compounds screened using the competitive ALPHAscreen, 106 compounds were identified as putative inhibitors of Zika E and advanced to antiviral testing. Following successive tests for antiviral activity in the plaque reduction by neutralization test ($PRNT_{50}$) and single-cycle infectivity experiments, seven lead compounds were advanced for further characterization.

with anti-ZIKV activity.

To prioritize compounds for follow-up studies, we also assessed antiviral potency by quantifying inhibition of ZIKV at 30 μM (compound:target ~ 10^4:1) in a single-cycle infectivity assay in which we made the assay conditions more stringent by increasing the viral inoculum to achieve MOI of 1 and also increasing the concentration of serum present during the inhibitor treatment from ~0.005% ($PRNT_{50}$) to ~0.1% (infectivity assay) (Fig. 3A). Only seven compounds were observed to inhibit ZIKV infectivity by more than 90% under these conditions using ~200-fold increase in challenge virus (Supporting Table 1). We note that the majority of the other ninety active compounds identified in primary screening exhibit potent and reproducible antiviral activity under less challenging conditions (*e.g.* $PRNT_{50}$) in which MOI and target abundance are lower. While we view many of these compounds as candidates for medicinal chemistry optimization, here we initially focused our efforts on the seven compounds with potent antiviral activity in the more stringent infectivity assay conducted at high target abundance. These seven compounds include three structurally related linear compounds and four distinct macrocycles (Fig. 3B and C).

We first determined the IC_{90}, defined as the compound concentration at which the infectious virus was decreased 1-log_{10} in the single-cycle infectivity assay (Fig. 3A). IC_{90} values ranged from 5.2 μM for LAS 52154459 to 20.3 μM for LAS 52154463 (Fig. 3B and Table 1). Notably, these compounds have antiviral potencies that are equal to or greater in potency than previously identified Zika E inhibitors (de Wispelaere et al., 2018). We counter-screened against cytotoxicity using a commercially available assay to determine the concentration-dependent effects of these compounds on cell viability. Although two compounds, LAS 52509955 and LAS 51635112, cause significant loss of cell viability at concentrations below 50 μM (Table 1), all compounds except LAS 52509955 have selectivity indices (IC_{90}/CC_{50}) greater than 5. This taken with the fact that the conditions used for the infectivity and $PRNT_{50}$ assays have a limited window of inhibitor treatment of one

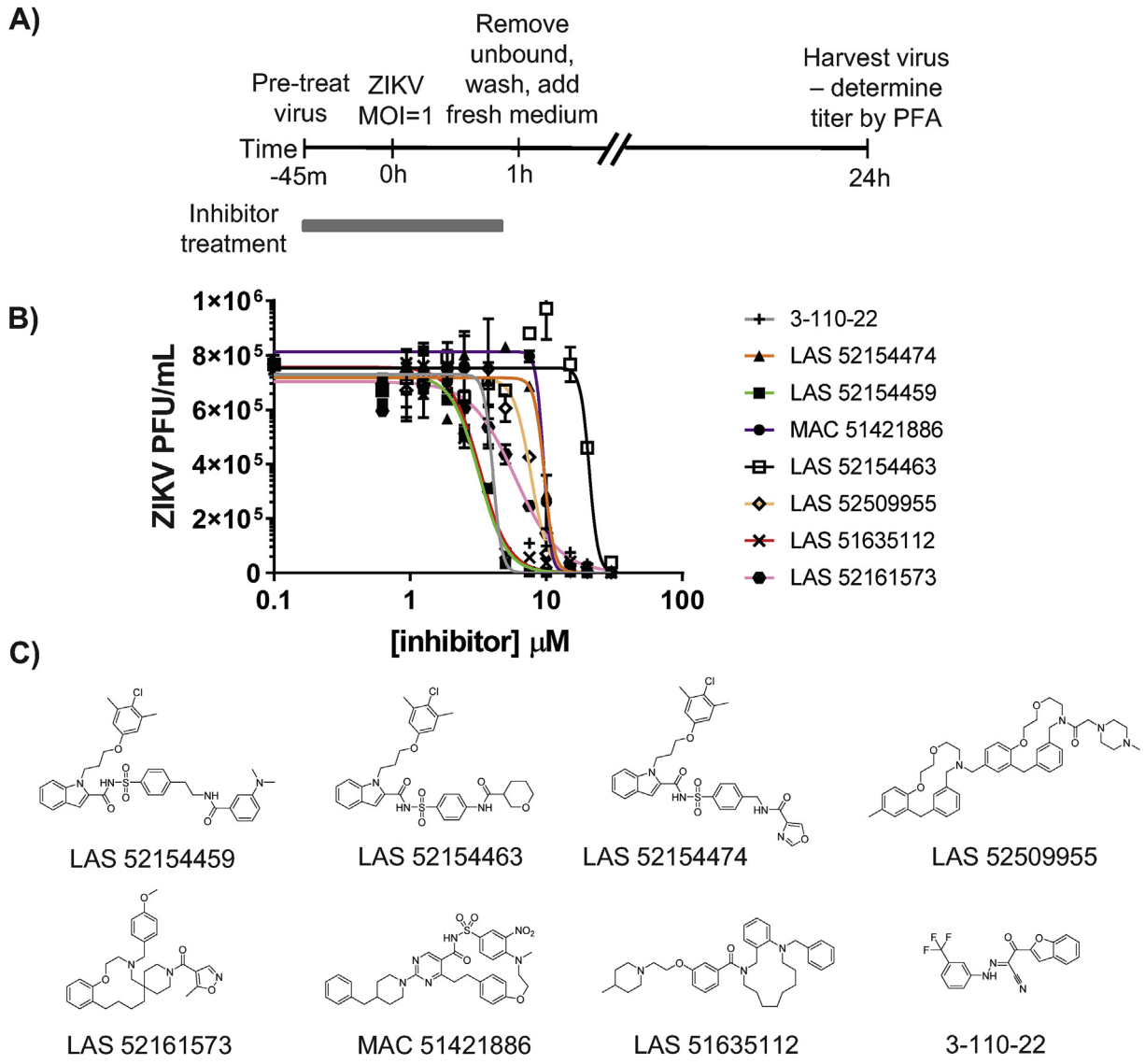

Fig. 3. Antiviral activity of lead compounds against Zika virus. (A) Schematic representation of the single-cycle infectivity assay utilized to determine the antiviral IC_{90} of the 7 lead compounds against ZIKV. **(B)** The production and release of infectious virus at 24 h post infection was determined by plaque formation assay (PFA) and plotted versus log_{10} inhibitor concentration. The anti-ZIKV IC_{90} value of each of the lead compounds was determined by non-linear regression analysis. The graph shown is representative of $n \geq 2$ independent experiments; error bars represent the standard deviation of the technical replicates within the experiment. The reported IC_{90} values are the average of $n \geq 2$ independent experiments performed for each compound. **(C)** Structures of the seven most potent inhibitors of ZIKV, which were selected for further characterization, and 3-110-22, the positive control..

Table 1
Summary of lead compound characterization. Luminescence data in the Zika sE ALPHAscreen were plotted as a function of compound concentration. IC_{50} values, defined as the concentration at which the signal is reduced to 50% of the DMSO control, were determined by non-linear regression analysis of the data. ZIKV $PRNT_{50}$ values were determined by non-linear regression analysis of data from the plaque reduction by neutralization test ($PRNT_{50}$) (Supp. Fig 1). Antiviral IC_{90} values were determined by non-linear regression analysis of data generated using the viral infectivity assay as shown in Fig. 3A and B. CC_{50} values correspond to the concentration of inhibitor at which a 50% reduction in viability of Vero cells is observed. A selectivity index corresponding to the ratio of CC_{50} and antiviral IC_{90} values is reported. DENV2 IC_{90} and VSV $PRNT_{50}$ values were determined in experiments analogous to the ZIKV single-cycle infectivity and $PRNT_{50}$ assays, respectively. All values are the average and standard deviation of $n \geq 2$ independent experiments.

Molecule Name	ALPHA IC_{50}, μM	ZIKV $PRNT_{50}$, μM	ZIKV IC_{90}, μM	CC_{50}, μM	Selectivity Index CC_{50}/IC_{90}	Avg. DENV2 IC_{90}, μM	VSV $PRNT_{50}$, μM
LAS 52154459	4.0 ± 4.5	< 0.9375	5.1 ± 0.3	98.11 ± 2.7	19	3.2 ± 1.8	5.1 ± 2.5
LAS 52509955	0.9 ± 0.06	1.4 ± 0.5	10.6 ± 0.2	15.9 ± 5.2	1.5	4.1 ± 1.1	3.9 ± 0.07
MAC 51421886	3.3 ± 2.7	1.7 ± 0.3	10.6 ± 0.6	> 100	> 10	3.8 ± 0.9	6.5 ± 0.7
LAS 52161573	4.2 ± 1.9	1.1 ± 0.2	11.4 ± 2.8	> 100	> 7.5	7.2 ± 2.5	2.9 ± 0.4
LAS 52154463	19.3 ± 15.3	7.4 ± 0.1	20.3 ± 5.9	> 100	> 5	7.9 ± 3.2	26.7 ± 4.7
LAS 51635112	3.8 ± 2.0	1.1 ± 0.3	7.8 ± 3.1	30 ± 2.5	5	2.5 ± 0.1	26.3 ± 5.2
LAS 52154474	18.4 ± 12.5	6.7 ± 0.1	11.0 ± 0.9	> 100	> 9	4.8 ± 2.8	17.9 ± 3.9

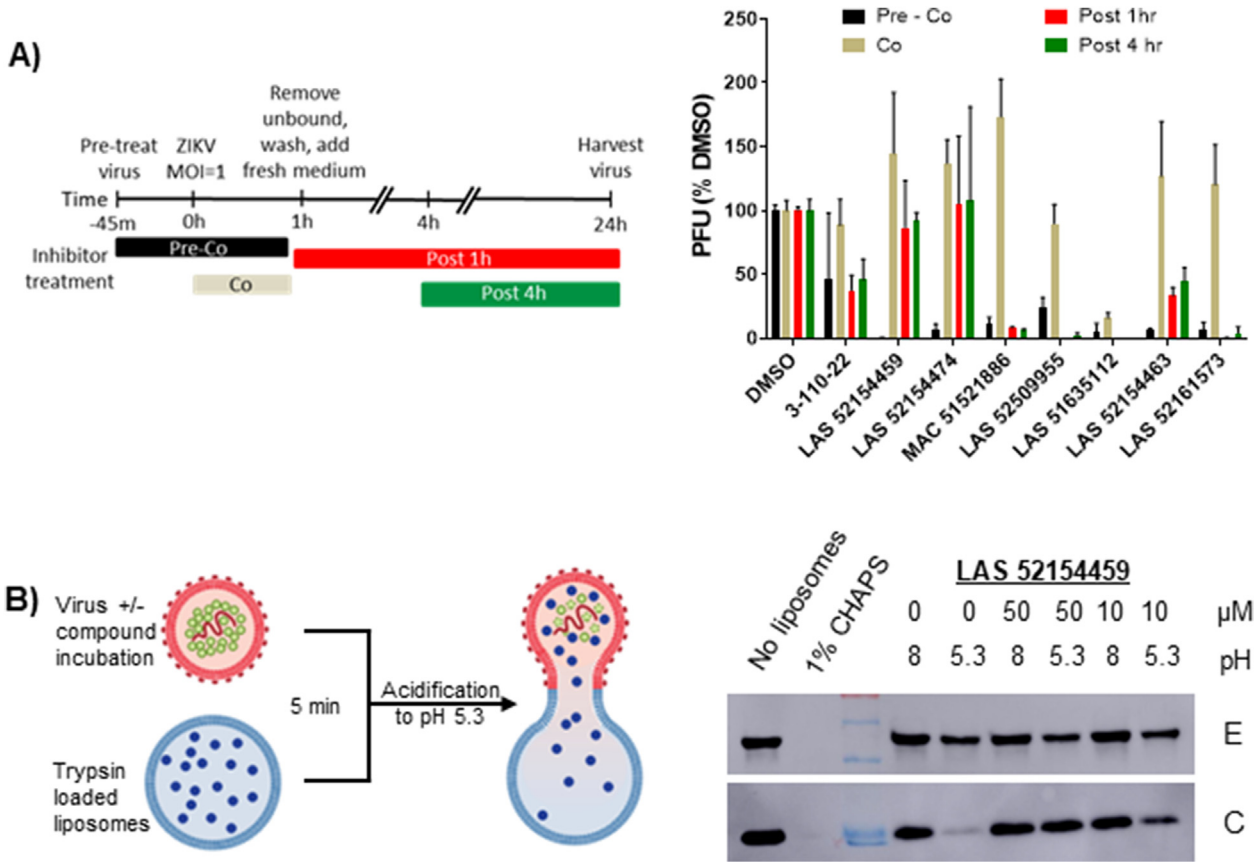

Fig. 4. Validation of ZIKV sE as the target of compound mediated anti-viral activity. (A) (*left*) Schematic of the time-of-addition study with boxes indicating when inhibitor (at the IC_{90} concentration) was incubated with virus for each of the conditions: pre-co infection, co (concurrent) alone, one hour post-infection, or four hour post-infection. Inhibitor concentrations corresponded to the antiviral IC_{90} measured in the infectivity assay as depicted in Fig. 3A and reported in Table 1. (*right*) Single-cycle viral yield was determined for all samples in the time-of-addition study by viral plaque formation assay of the supernatants at 24 hours post-infection. Data are normalized to the DMSO-control. All compounds exhibit approximately 1-log_{10} unit decrease when present prior to and during the infection ("pre-co" conditions) as expected. Except for LAS 51635112, this antiviral activity is lost when inhibitor treatment is limited to the one hour infection period ("co" condition). Additional antiviral activity is observed for many of the compounds when added post-infection, which may reflect inhibition of E during virion morphogenesis or antiviral activity mediated by a target other than Zika sE. The graph shown is an average of 2 biological replicates, each performed with 2 technical duplicates. Error bars represent standard deviation of the biological replicates. **(B)** (*left*) Schematic of the capsid protection assay to monitor E-mediated membrane fusion. Acidification of mixtures of DENV2 virions with trypsin-loaded liposomes results in fusion of the two membranes, which enables trypsin-mediated digestion of the DENV2 capsid protein (C) while E on the exterior of the viral lipid bilayer remains intact. Inhibition of DENV2 E-mediated fusion results in protection of the C protein. (*right*) Western blot analyses of the DENV2 E and C proteins are shown for fusion reactions performed as described in the schematic in the absence or presence of 10 µM or 50 µM of compound LAS 52154459. Reactions performed at pH 5.5 in the absence of inhibitor show digestion of C, indicating viral fusion with the trypsin-loaded liposome. LAS 52154459 exhibits concentration-dependent protection of DENV2 C indicating inhibition of fusion. Blots shown are representative of 2 independent experiments. Note that the ratio of target:inhibitor in this assay represents > 10-fold increase relative to that in the viral infectivity assay (Fig. 3) and > 200-fold increase in target abundance relative to the $PRNT_{50}$ assay.

hour during the initial infection indicate that general cytotoxicity is unlikely to contribute to the observed antiviral activity.

To verify that inhibition of viral entry is the mode of action of these compounds, we performed a series of time-of-addition experiments. Using final concentrations corresponding to the previously determined IC_{90} values, inhibitors were 1) pre-incubated with viral inoculum and present during infection (repeating the infectivity assay), 2) only present during the one hour infection with cells, or 3) added at either one hour or four hours post infection (Fig. 4A). We quantified viral yield for all samples at 24 hours post-infection by viral plaque formation assay. As expected, compounds reduced viral yield ~1-log_{10} after pre-incubation with the inhibitor, while all compounds except LAS 51635112 had minimal activity when added concurrent with infection, presumably due to limited time for target engagement. We observed additional antiviral activity for four of the compounds when they were delivered post-infection (Fig. 4A), indicating that these compounds may additionally inhibit the function of Zika E during virion morphogenesis and/or egress or may have antiviral activity mediated by other targets. In contrast, the 3 linear compounds (LAS 52154459, LAS 52154463, and LAS 52154474) exhibit only very modest inhibition when added post-infection, consistent with inhibition of E during viral entry as the primary antiviral mode of action of these compounds.

To assess the selectivity of these ZIKV inhibitors, we examined them for activity against DENV2, a related flavivirus, as well as against vesicular stomatitis virus (VSV), an unrelated, enveloped virus. Using the more stringent infectivity assay (MOI 1) to quantify anti-DENV2 activity, we observed IC_{90} values < 5 µM. This is somewhat unexpectedly on average 3- to 4-fold more potent inhibition of DENV2 over ZIKV (Table 1). We hypothesize that this may reflect increased "breathing" activity of the viral particle of DENV as compared to ZIKV (Dowd et al., 2015; Kostyuchenko et al., 2016; Sirohi et al., 2016), which may affect accessibility of the pocket between domains I and II of E in which these compounds likely bind. A second potential reason for the reduced activity against ZIKV is suggested by the recent report that ZIKV entry can be mediated by alternative pathways independent of receptor binding and acidification (Rawle et al., 2018). Although all seven compounds

exhibit modest inhibition of VSV in $PRNT_{50}$ assays, the antiviral potency is significantly less than observed against ZIKV. Together, these data indicate that these compounds have some level of specificity for ZIKV, DENV2, and perhaps other related flaviviruses.

Due to the increased potency of the compounds against DENV2, we sought to further establish the mechanism of action with the representative compound LAS 52154459 on DENV2 E-mediated membrane fusion using a biochemical assay in which acidic pH triggers E-mediated fusion of virions with trypsin-encapsulating liposomes and leads to proteolytic digestion of the viral capsid protein (C) (Fig. 4B). Inhibition of E-mediated fusion results in protection of DENV2C from digestion in this assay. Following incubation of DENV2 virions with LAS 52154459, we observed concentration-dependent (compound:-target ~ 10^3:1 at 50 μM) protection of viral capsids from proteolysis after acidification of the solution to pH 5.5 (Fig. 4B). This demonstrates that LAS 52154459 prevents virion-liposome membrane fusion and formation of a functional pore in this assay, consistent with the idea that the ALPHAscreen identifies direct-acting antivirals that inhibit membrane fusion mediated by the flavivirus E protein.

In summary, we have established and validated the first target-based assay to identify direct-acting antivirals of Zika E. Our results suggest the feasibility of developing analogous assays for additional flavivirus E proteins. Such parallel assays could be very useful in identification and development of antivirals with broad-spectrum activity. In the pilot high-throughput screen conducted for this study, we identified seven new lead compounds and characterized their antiviral activity against ZIKV and DENV2. The most promising of these seven compounds are a set of three structurally related linear compounds, LAS 52154459, LAS 52154463, and LAS 52154474 (Fig. 3C), all of which exhibit minimal toxicity and act predominantly on the entry process based upon our time-of-addition experiments. We note that several additional structurally related linear compounds were present in the screen, and most were also identified as “hit” compounds in the ALPHAscreen. Follow up work on these additional compounds and medicinal chemistry efforts to define structure-activity-relationships (SAR) driving antiviral potency and selectivity against ZIKV, DENV2, and potentially other flaviviruses will be an essential part of efforts to evaluate and optimize direct-acting antivirals against this target class.

Acknowledgements

Special thanks to Jennifer Smith and the ICCB-Longwood Screening Facility staff for access to the screening compounds, instrumentation, and technical support. We would also like to thank the following colleagues for sharing reagents: Lee Gehrke for the DENV2 New Guinea C strain virus; Didier Musso and Nathalie Pardigon for ZIKV PF13-251013-18 strain; Sean Whelan for VSV; Katya Heldwein for S2 cells; and Eva Harris for BHK-21 cells. The office of Congressman Michael Capuano is thanked for assistance in importing ZIKV. The work in this manuscript has been supported by the Blavatnik Biomedical Accelerator and National Institutes of Health award U19AI109740.

Appendix A. Supplementary data

Supplementary data to this article can be found online at https://doi.org/10.1016/j.antiviral.2019.02.008.

References

Boldescu, V., Behnam, M.A.M.A., Vasilakis, N., Klein, C.D., 2017. Broad-spectrum agents for flaviviral infections: dengue, Zika and beyond. Nat. Rev. Drug Discov. 16, 565–586.

Calvet, G.A., Kara, E.O., Giozza, S.P., Bôtto-Menezes, C.H.A.H., Gaillard, P., Oliveira Franca, R.F., de Lacerda, M.V.G.V. de, Costa Castilho, M. da, Brasil, P., Sequeira, P.C.C. de, Mello, M.B. de, Bermudez, X.P.D.P., Modjarrad, K., Meurant, R., Landoulsi, S., Benzaken, A.S., Filippis, A.M.B.M. de, Broutet, N.J.N.J., 2018. Study on the persistence of Zika virus (ZIKV) in body fluids of patients with ZIKV infection in Brazil. BMC Infect. Dis. 18, 49.

Capeding, M.R., Tran, N.H., Hadinegoro, S.R., Ismail, H.I., Chotpitayasunondh, T., Chua, M.N., Luong, C.Q., Rusmil, K., Wirawan, D.N., Nallusamy, R., Pitisuttithum, P., Thisyakorn, U., Yoon, I.-K.K., Vliet, D. van der, Langevin, E., Laot, T., Hutagalung, Y., Frago, C., Boaz, M., Wartel, T.A., Tornieporth, N.G., Saville, M., Bouckenooghe, A., 2014. Clinical efficacy and safety of a novel tetravalent dengue vaccine in healthy children in Asia: a phase 3, randomised, observer-masked, placebo-controlled trial. Lancet 384, 1358–1365.

Clark, M.J., Miduturu, C., Schmidt, A.G., Zhu, X., Pitts, J.D., Wang, J., Potisopon, S., Zhang, J., Wojciechowski, A., Hann Chu, J.J., Gray, N.S., Yang, P.L., 2016. GNF-2 inhibits dengue virus by targeting Abl kinases and the viral E protein. Cell. Chem. Biol. 23, 443–452.

de Wispelaere, M., Lian, W., Potisopon, S., Li, P.-C.C., Jang, J., Ficarro, S.B., Clark, M.J., Zhu, X., Kaplan, J.B., Pitts, J.D., Wales, T.E., Wang, J., Engen, J.R., Marto, J.A., Gray, N.S., Yang, P.L., 2018. Inhibition of flaviviruses by targeting a conserved pocket on the viral envelope protein. Cell. Chem. Biol. 25, 1006–1016 e8.

Dowd, K.A., DeMaso, C.R., Pierson, T.C., 2015. Genotypic differences in dengue virus neutralization are explained by a single amino acid mutation that modulates virus breathing. mBio 6 e01559–15.

Fowler, A.M., Tang, W.W., Young, M.P., Mamidi, A., Viramontes, K.M., McCauley, M.D., Carlin, A.F., Schooley, R.T., Swanstrom, J., Baric, R.S., Govero, J., Diamond, M.S., Shresta, S., 2018. Maternally acquired Zika antibodies enhance dengue disease severity in mice. Cell Host Microbe 24, 743–750 e5.

Gaudinski, M.R., Houser, K.V., Morabito, K.M., Hu, Z., Yamshchikov, G., Rothwell, R.S., Berkowitz, N., Mendoza, F., Saunders, J.G., Novik, L., Hendel, C.S., Holman, L.A., Gordon, I.J., Cox, J.H., Edupuganti, S., McArthur, M.A., Rouphael, N.G., Lyke, K.E., Cummings, G.E., Sitar, S., Bailer, R.T., Foreman, B.M., Burgomaster, K., Pelc, R.S., Gordon, D.N., DeMaso, C.R., Dowd, K.A., Laurencot, C., Schwartz, R.M., Mascola, J.R., Graham, B.S., Pierson, T.C., Ledgerwood, J.E., Chen, G.L., 2018. Safety, tolerability, and immunogenicity of two Zika virus DNA vaccine candidates in healthy adults: randomised, open-label, phase 1 clinical trials. Lancet 391, 552–562.

Govero, J., Esakky, P., Scheaffer, S.M., Fernandez, E., Drury, A., Platt, D.J., Gorman, M.J., Richner, J.M., Caine, E.A., Salazar, V., Moley, K.H., Diamond, M.S., 2016. Zika virus infection damages the testes in mice. Nature 540, 438–442.

Hadinegoro, S.R., Arredondo-García, J.L., Capeding, M.R., Deseda, C., Chotpitayasunondh, T., Dietze, R., Muhammad Ismail, H.I., Reynales, H., Limkittikul, K., Rivera-Medina, D.M., Tran, H.N., Bouckenooghe, A., Chansinghakul, D., Cortés, M., Fanouillere, K., Forrat, R., Frago, C., Gailhardou, S., Jackson, N., Noriega, F., Plennevaux, E., Wartel, T.A., Zambrano, B., Saville, M., 2015. Efficacy and long-term safety of a dengue vaccine in regions of endemic disease. N. Engl. J. Med. 373, 1195–1206.

Halstead, S.B., 2016. Critique of World Health Organization recommendation of a dengue vaccine. J. Infect. Dis. 214, 1793–1795.

Halstead, S.B., Russell, P.K., 2016. Protective and immunological behavior of chimeric yellow fever dengue vaccine. Vaccine 34, 1643–1647.

Hamel, R., Dejarnac, O., Wichit, S., Ekchariyawat, P., Neyret, A., Luplertlop, N., Perera-Lecoin, M., Surasombatpattana, P., Talignani, L., Thomas, F., Cao-Lormeau, V.-M.M., Choumet, V., Briant, L., Desprès, P., Amara, A., Yssel, H., Missé, D., 2015. Biology of Zika virus infection in human skin cells. J. Virol. 89, 8880–8896.

Kostyuchenko, V.A., Lim, E.X., Zhang, S., Fibriansah, G., Ng, T.-S.S., Ooi, J.S., Shi, J., Lok, S.-M.M., 2016. Structure of the thermally stable Zika virus. Nature 533, 425–428.

Lian, W., Jang, J., Potisopon, S., Li, P.-C.C., Rahmeh, A., Wang, J., Kwiatkowski, N.P., Gray, N.S., Yang, P.L., 2018. Discovery of immunologically inspired small molecules that target the viral envelope protein. ACS Infect. Dis. 4, 1395–1406.

Lim, S.P., 2019. Dengue drug discovery: progress, challenges and outlook. Antiviral Res. 163, 156–178.

Ma, W., Li, S., Ma, S., Jia, L., Zhang, F., Zhang, Y., Zhang, J., Wong, G., Zhang, S., Lu, X., Liu, M., Yan, J., Li, W., Qin, C., Han, D., Qin, C., Wang, N., Li, X., Gao, G.F., 2016. Zika virus causes testis damage and leads to male infertility in mice. Cell 167, 1511–1524 e10.

Modjarrad, K., Lin, L., George, S.L., Stephenson, K.E., Eckels, K.H., La Barrera, R.A. De, Jarman, R.G., Sondergaard, E., Tennant, J., Ansel, J.L., Mills, K., Koren, M., Robb, M.L., Barrett, J., Thompson, J., Kosel, A.E., Dawson, P., Hale, A., Tan, C.S., Walsh, S.R., Meyer, K.E., Brien, J., Crowell, T.A., Blazevic, A., Mosby, K., Larocca, R.A., Abbink, P., Boyd, M., Bricault, C.A., Seaman, M.S., Basil, A., Walsh, M., Tonwe, V., Hoft, D.F., Thomas, S.J., Barouch, D.H., Michael, N.L., 2018. Preliminary aggregate safety and immunogenicity results from three trials of a purified inactivated Zika virus vaccine candidate: phase 1, randomised, double-blind, placebo-controlled clinical trials. Lancet 391, 563–571.

Pan-American Health Organization/World Health Organization Zika Report https://www.paho.org/hq/index.php?option=com_content&view=article&id=11599:regional-zika-epidemiological-update-americas&Itemid=41691&lang=en.

Paz-Bailey, G., Rosenberg, E.S., Doyle, K., Munoz-Jordan, J., Santiago, G.A., Klein, L., Perez-Padilla, J., Medina, F.A., Waterman, S.H., Gubern, C.G., Alvarado, L.I., Sharp, T.M., 2017. Persistence of Zika virus in body fluids - preliminary report. N. Engl. J. Med. 379 (13), 1234–1243.

Rawle, R.J., Webster, E.R., Jelen, M., Kasson, P.M., Boxer, S.G., 2018. pH dependence of Zika membrane fusion kinetics reveals an off-pathway state. ACS Cent. Sci. 4, 1503–1510.

Sabchareon, A., Wallace, D., Sirivichayakul, C., Limkittikul, K., Chanthavanich, P., Suvannadabba, S., Jiwariyavej, V., Dulyachai, W., Pengsaa, K., Wartel, T.A., Moureau, A., Saville, M., Bouckenooghe, A., Viviani, S., Tornieporth, N.G., Lang, J., 2012. Protective efficacy of the recombinant, live-attenuated, CYD tetravalent dengue vaccine in Thai schoolchildren: a randomised, controlled phase 2b trial. Lancet 380, 1559–1567.

Sapparapu, G., Fernandez, E., Kose, N., Cao, Bin, Fox, J.M., Bombardi, R.G., Zhao, H.,

Nelson, C.A., Bryan, A.L., Barnes, T., Davidson, E., Mysorekar, I.U., Fremont, D.H., Doranz, B.J., Diamond, M.S., Crowe, J.E., 2016. Neutralizing human antibodies prevent Zika virus replication and fetal disease in mice. Nature 540, 443–447.

Schmidt, A.G., Lee, K., Yang, P.L., Harrison, S.C., 2012. Small-molecule inhibitors of dengue-virus entry. PLoS Pathog. 8, e1002627.

Sirohi, D., Chen, Z., Sun, L., Klose, T., Pierson, T.C., Rossmann, M.G., Kuhn, R.J., 2016. The 3.8 Å resolution cryo-EM structure of Zika virus. Science 352, 467–470.

Stettler, K., Beltramello, M., Espinosa, D.A., Graham, V., Cassotta, A., Bianchi, S., Vanzetta, F., Minola, A., Jaconi, S., Mele, F., Foglierini, M., Pedotti, M., Simonelli, L., Dowall, S., Atkinson, B., Percivalle, E., Simmons, C.P., Varani, L., Blum, J., Baldanti, F., Cameroni, E., Hewson, R., Harris, E., Lanzavecchia, A., Sallusto, F., Corti, D., 2016. Specificity, cross-reactivity, and function of antibodies elicited by Zika virus infection. Science 353, 823–826.

Tassaneetrithep, B., Burgess, T.H., Granelli-Piperno, A., Trumpfheller, C., Finke, J., Sun, W., Eller, M.A., Pattanapanyasat, K., Sarasombath, S., Birx, D.L., Steinman, R.M., Schlesinger, S., Marovich, M.A., 2003. DC-SIGN (CD209) mediates dengue virus infection of human dendritic cells. J. Exp. Med. 197, 823–829.

Villar, L., Dayan, G.H., Arredondo-García, J.L.L., Rivera, D.M., Cunha, R., Deseda, C., Reynales, H., Costa, M.S., Morales-Ramírez, J.O., Carrasquilla, G., Rey, L.C., Dietze, R., Luz, K., Rivas, E., Miranda Montoya, M.C., Cortés Supelano, M., Zambrano, B., Langevin, E., Boaz, M., Tornieporth, N., Saville, M., Noriega, F., 2015. Efficacy of a tetravalent dengue vaccine in children in Latin America. N. Engl. J. Med. 372, 113–123.

Zimmerman, M.G., Quicke, K.M., O'Neal, J.T., Arora, N., Machiah, D., Priyamvada, L., Kauffman, R.C., Register, E., Adekunle, O., Swieboda, D., Johnson, E.L., Cordes, S., Haddad, L., Chakraborty, R., Coyne, C.B., Wrammert, J., Suthar, M.S., 2018. Cross-reactive dengue virus antibodies augment Zika virus infection of human placental macrophages. Cell Host Microbe 24, 731–742 e6.